Circadian stimulus – A computation model with photometric and colorimetric quantities

W Truong MSc[a,b] ⬤, **V Trinh** Dr-Ing[b] ⬤ and **TQ Khanh** Dr-Ing. habil[b]
[a]Department of Research & Development, PRACHT Institute of Technology, Dautphetal-Buchenau, Germany
[b]Laboratory of Lighting Technology, Technische Universität Darmstadt, Darmstadt, Germany

The circadian stimulus is an important, validated and updated metric that describes the invisible influences of light on the human circadian system explicitly and scientifically. However, an absolute spectral power distribution must be supplied for its computation, which is only measurable by an expensive and complicated spectrometer. This paper proposes an alternative circadian stimulus computation model that is identified as the function $CS(z, E_v)$ for white light sources based on the most common and simplest parameters of illuminance E_v in lux and the chromaticity coordinate z. These parameters are well known and widely used in both colour science and lighting technology. In order to prove the accuracy and availability of the model, an internal validation was performed with the adapted method repeating split data to check the goodness of the model fit. The fitted model achieved a maximum residual of 0.058 in the circadian stimulus quantity ($R^2 = 0.998$). An external validation with the maximum residual of 0.030 ($R^2 = 0.999$) provided stronger evidence for the usability of the model in applications.

1. Introduction

Today, lighting practitioners are mainly using photometric and colorimetric quantities, such as illuminance (E_v) in lux, correlated colour temperature (CCT) in degrees Kelvin (K), colour rendering index (R_a) and CIE visual angle $2°$ chromaticity coordinates x, y and z, to describe human visual performance.[1] In contrast to these visual metrics, the metrics relating to the non-visual effects of light have not been widely accepted. The International Commission on Illumination (CIE) has recently published a new metric system to describe the response of the five retinal photoreceptors to incident radiation.[2] In Germany, the DIN standards committee has introduced the melanopic factor of luminous radiation a_{mel}, melanopic daylight equivalent illuminance $E_{v,mel,D65}$ and design guidelines for biologically effective illumination.[3,4] The word '*melanopic*' refers to the effect of light on the intrinsically photosensitive retinal ganglion cells (ipRGC) containing the photopigment melanopsin. Additionally, Lucas *et al.*[5] recommended their metric system of α-opic lux for each photopigment to evaluate biological effects by light. Parallel to the metric systems of CIE, DIN and Lucas *et al.*, Rea *et al.* also developed the metric of circadian stimulus (*CS*) in 2005 (revised in 2010, 2012 and 2018)

Address for correspondence: W Truong, PIT GmbH – PRACHT Institute of Technology, Am Seerain 3, Dautphetal-Buchenau 35232, Germany.
E-mail: w.truong@pracht.com

to characterise the light impact on the circadian system.[6–9]

In the following, the different metric systems are discussed in detail. The DIN metric uses an action spectrum to describe the melanopic effect of light. This approach gives the lighting practitioners the quantities a_{mel} and $E_{v,mel,D65}$ to evaluate the relative spectral power distribution and the 'melanopic' illuminance.[3] However, the efficiency function is based on one photopigment and this would misrepresent the spectral sensitivity of the circadian system as it includes signals from the long-, medium-, and short-wavelength sensitive cone photoreceptors and the rod photoreceptors.[9] Similar to the DIN system, CIE and Lucas *et al.* have introduced five separate quantities for each retinal photoreceptor based on their photopigments.[2,5] This enables the evaluation of light effectiveness on each photoreceptor regardless of the neuroanatomy and neurophysiology of the rest of the circadian system. Thus, by using this metric system, lighting practitioners would have to work with five new parameters, which would not be practicable. In order to promote acceptance of a new metric system, a simpler approach is needed that takes into account the human neuroanatomy and neurophysiology.

In contrast to metric systems of CIE, DIN and Lucas *et al.*, the last revised metric CS_{2018} incorporates the neuroanatomy, neurophysiology and operational characteristics of the circadian system, which is the most accurate approach to describe the biological output of melatonin suppression and hence the human circadian system.[9] Similar to the CS, other biological outputs like brightness, visual clarity, colour preference and scene preference are more accurate if the neurophysiology or interaction between multiple retinal photoreceptors is considered.[10–13] Furthermore, lighting planning recommendations for academic and industrial purposes have been defined by thresholds of circadian-effective light (high: $CS_{2018} \geq 0.3$; low: $CS_{2018} \leq 0.15$).[9,14] The CS metric has been applied for lighting at workplaces and living spaces in several field studies.[15–17]

There is criticism about the application of CS_{2018} during daytime, as it describes the nocturnal melatonin suppression. But to suppress the melatonin secretion in the pineal gland, the light signal passes through the suprachiasmatic nucleus (SCN),[18] which is considered to be the main pacemaker of human endogenous circadian clock.[19] Light entrains the human circadian clock via the SCN and indirectly influences sleep quality and other biological circadian rhythms.[20] The human circadian system is light-sensitive for almost 24 h, with light sensitivity being phase-dependent on the internal clock. This sensitivity is described by phase response curves (PRCs).[21,22] Thus, the metric CS_{2018} also indirectly describes the light impact on the human circadian clock or the pacemaker SCN. The application of CS_{2018} thresholds during daytime would entrain humans to working times, which improves, indirectly, well-being and sleep quality.[16,17]

However, to compute CS_{2018}, a spectrometer or the non-commercially available daysimeter from Rea *et al.*[7] is required. Lighting practitioners need to invest in a portable spectrometer and implement the CS_{2018} formula to be able to evaluate the CS. The idea of this work is to analyse Rea's CS_{2018} model to create a model function solely dependent on generally accepted metrics. Hence, already existing common measurement equipment (e.g. tristimulus colorimeters) can be used by lighting practitioners and researchers to compute CS_{2018} and to verify lighting installations in the context of evaluation of the light impact on the circadian human system.

In the next section, a model function with the appropriate photometric and colorimetric quantities is established by using the spectra of 302 different white light sources. Afterwards both internal and external

validations are performed to verify the predictive quality of the model.

2. Model fitting and regression analysis

The aim of this work is to create a simple model function of CS_{2018} for lighting practitioners and researchers using common quantities. Illuminance E_v and chromaticity coordinates x,y,z (CIE, observation angle $2°$) are focused on as they are widely known and applied frequently in colour science and in the lighting industry.

First, the relative spectra of 302 measured white light sources are selected and listed in detail in Table 1. Non-white light sources are excluded, and the most common white light sources are used instead, as they make a major contribution to modern lighting systems. In this work, white light sources follow the CIE concept of CCT,[1] in which the chromaticity of the white light sources does not differ more than $\Delta uv = 5 \cdot 10^{-2}$ from the chromaticity of the Planckian radiator. The large number of LED light sources in Table 1 also proves their important role in current lighting applications. Second, an illuminance range with 19 steps from 10 lx to 10,000 lx (see equation (1)) is defined

$$E_v = 10^x \quad \text{with } x = \left\{ 1, \frac{7}{6}, \frac{8}{6}, \ldots, 4 \right\} \quad (1)$$

Table 1 Quantity and types of white light source used in this work with correlated colour temperature (2201 K–7898 K) and colour rendering index R_a (41–100)

| Ordinate	Type	Quantity
1	Conventional incandescent lamp	11
2	Compact fluorescent lamps	4
3	Semi-compact fluorescent lamps	6
4	Fluorescent tubes	32
5	LED lamps	166
6	LED luminaires	83

Third, the illuminance range is applied to the 302 relative spectra, resulting in 5738 absolute spectra (302 light sources × 19 steps). Finally, CS_{2018}, E_v, x, y and z are calculated from these absolute spectra.

The chromaticity coordinates are then computed from the relative spectral power distribution of the light sources. Then, the three chromaticity coordinates and illuminance can be multiplied by each other, such as $(x \cdot E_v)$, $(y \cdot E_v)$ or $(z \cdot E_v)$ to consider the effect of both the absolute amount of light and the spectral geometry in different wavelength ranges.
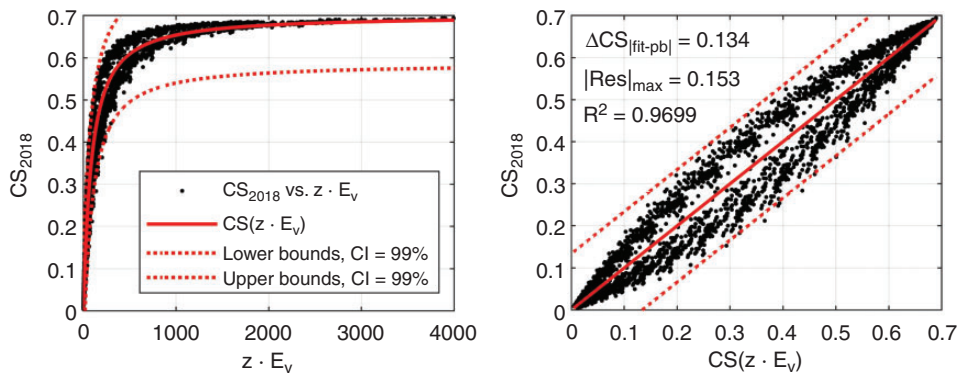
The relationship between CS_{2018}, $(x \cdot E_v)$, $(y \cdot E_v)$ and $(z \cdot E_v)$, illustrated in Figures 1 and 2 (The left image, respectively) shows that the distribution with the product $(z \cdot E_v)$ has the lowest data point scatter compared to the distribution with $(x \cdot E_v)$ and $(y \cdot E_v)$. Therefore, $(z \cdot E_v)$ is the best solution to fit a model function in terms of accuracy. Consequently, a fitting equation (2) based on Rea's CL_A and CS formula is proposed as follows (also see equations (1) and (2) in Rea and Figueiro's work[9]).

$$CS(z \cdot E_v) = 0.7 - \frac{0.7}{1 + a \cdot (z \cdot E_v)^b} \quad (2)$$

Now the curve fitting is performed, using the non-linear least squares (NLLS) method to determine the fitting parameters a, b in equation (2). The fit function $CS(z \cdot E_v)$ and the lower and upper prediction bounds with 99% confidence interval are shown in Figure 2. This visually indicates that the fitted function with '*all values*' is not accurate enough. This is also confirmed by the difference between the fit and the prediction bounds (pb) $\Delta CS_{|fit-pb|} = 0.134$ and the maximum absolute residual $|Res|_{max} = 0.153$, which are relatively large errors compared to the proposed threshold of the circadian effective light levels proposed by
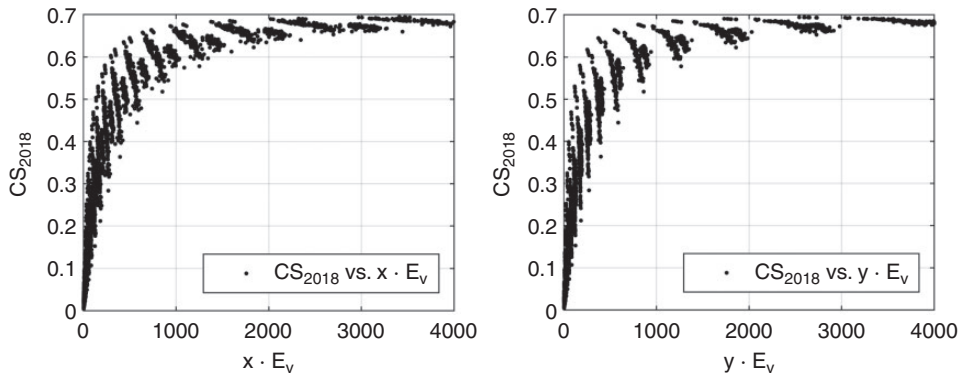
Figure 1 Scatter plots CS_{2018} vs. $(x \cdot E_v)$ (left) and CS_{2018} vs. $(y \cdot E_v)$ (right) with 5738 data points

Figure 2 Left: Relationship between CS_{2018} and $z \cdot E_v$ ($n = 5738$) is fitted on equation (2) resulting to fitting parameters a, b, lower and upper prediction bounds with 99% confidence interval (CI). Right: Relationship between CS_{2018} and fitted model function $CS(z \cdot E_v)$ with prediction bounds, coefficient of determination R^2, difference between fit and prediction bounds $\triangle CS_{|fit\text{-}pb|}$ and maximum absolute residual $|Res|_{max}$. (For more detailed values see Table 2, 'all values')

Figueiro *et al.*[14] Notably, both $\triangle CS_{|fit\text{-}pb|}$ and $|Res|_{max}$ have both the same unit as CS_{2018}. The maximum absolute residual represents the maximum deviance between CS_{2018} and $CS(z \cdot E_v)$ in units of CS.

A closer inspection of the relationship between CS_{2018} and $CS(z \cdot E_v)$ in Figure 2 shows that the fitted data seem to follow two distinct functions. This distinct characteristic arises from Rea's original formula circadian light (CL_A), which uses a corresponding if-condition SV to separate spectra, see equation (3). Thus, the prediction accuracy can be

improved if Rea's if-condition SV can be replaced by an if-condition of z. This idea is very interesting and motivated, because on the one side it helps the proposed model to become more accurate and on the other side it can reflect 100% the explicit nature of the original model of Rea *et al.*[8,9] with its if-condition.

2.1 The if-condition of z

Originally, the if-condition SV was developed to distinguish between the '*blue signal*' and '*yellow signal*' of light.[9] Mathematically,

equation (3) is only discriminating between the positive and negative values. In equation (3), λ is the wavelength of electromagnetic radiation in nm, S_λ/mp_λ is the S-cone fundamental weighted with the macular pigment transmittance, E_λ is the spectral irradiance distribution and V_λ is the photopic luminous efficiency function. In this calculation, only the relative spectral power distribution is taken into consideration. This leads to the idea of finding a relationship between SV and the chromaticity coordinate z to improve the proposed model in equation (2).

$$SV = \int \frac{S_\lambda}{mp_\lambda} E_\lambda \mathrm{d}\lambda - k \int \frac{V_\lambda}{mp_\lambda} E_\lambda \mathrm{d}\lambda \qquad (3)$$

By using equation (3), SV values were computed from the 5738 absolute spectra and are illustrated in Figure 3. It can be observed that all positive SV values are in the first quadrant and all negative SV values are in the third quadrant. Thus, a simple if-condition $(0.195 - z)$ is able to replicate the spectral separation of the if-condition SV. Notably, the vertical line at $z = 0.195$ is found arbitrarily between the last negative and the first positive SV values.

Applying the if-condition $(0.195 - z)$, the original 5738 data points are divided into group 'g1' and group 'g2':

g1: $(z > 0.195) \triangleq (SV > 0)$, quantity: 3097
g2: $(z \leq 0.195) \triangleq (SV \leq 0)$, quantity: 2641

For both groups, the NLLS fitting was performed based on equation (2). The fitting results are illustrated in Figure 4. The two distinct distributions in Figure 2 are clearly separated into group 'g1' and group 'g2'. Additionally, to compare fits of '*all values*' with 'g1' and 'g2', fitting parameters a and b, sum of squared error SSE, coefficient of determination R^2, adjusted R-square $_{adj}R^2$, root mean squared error $RMSE$, $\Delta CS_{|fit-pb|}$ and $|Res|_{max}$ are shown in Table 2.

All performance measures (SSE, R^2, $_{adj}R^2$, $RMSE$, $\Delta CS_{|fit-pb|}$, $|Res|_{max}$) are indicating an improvement of the fit. The prediction parameters $\Delta CS_{|fit-pb|}$ and $|Res|_{max}$ for 'g1' and 'g2' are smaller (more accurate) than the parameters for '*all values*'. However, the prediction of 'g1' (see Figure 4, $\Delta CS_{|fit-pb|} = 0.065$ and $|Res|_{max} = 0.114$) is still inaccurate. Therefore, the improvement for this group should be further investigated in order to meet the requirement for higher accuracy.
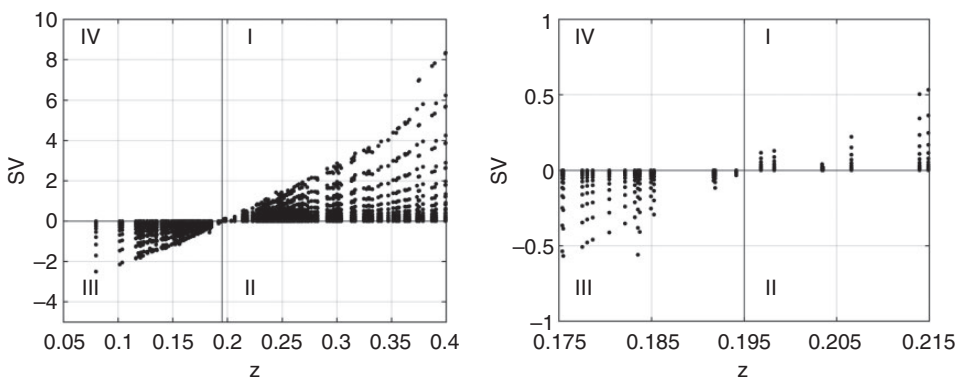
Figure 3 Left: Relationship between SV and z values. Positive SV values are located in the first quadrant and negative values are located in the third quadrant ($n = 5738$). Right: Vertical line at ($z = 0.195$) and the x-axis are separating positive and negative SV values
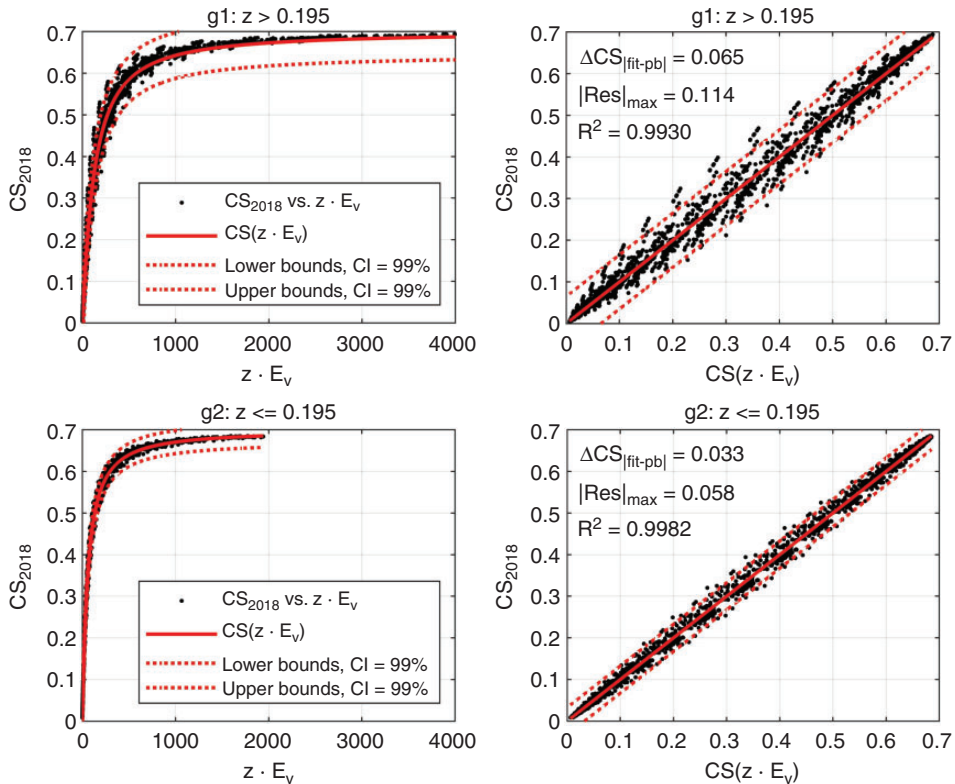
Figure 4 Scatter plots with model function CS($z \cdot E_v$) and prediction bounds representing group g1 (upper images, $n = 3097$) and group g2 (lower images, $n = 2641$). The regression analysis parameters can be found in Table 2

Table 2 Fitting parameters, performance measures for fitting conditions 'all values', 'g1', 'g2', 'g1a' and 'g2a'

Parameter	All values	g1: $z > 0.195$	g2: $z \leq 0.195$	g1a: $z > 0.195$	g2a: $z \leq 0.195$
a	0.007850	0.004060	0.011376	0.016781	0.004893
b	1.085174	1.147418	1.099980	2.268904	0.656298
c	–	–	–	0.509265	1.677749
SSE	11.147452	1.418231	0.304258	0.356801	0.185135
R^2	0.969916	0.993008	0.998183	0.998241	0.998895
$_{adj}R^2$	0.969911	0.993006	0.998183	0.998240	0.998894
$RMSE$	0.044084	0.021406	0.010737	0.010739	0.008377
$\Delta CS_{|fit-pb|}$	0.134	0.065	0.033	0.036	0.028
$|Res|_{max}$	0.154	0.114	0.058	0.052	0.052

Note: Fitting 'all values', 'g1' and 'g2' was based on equation (2) and fitting 'g1a' and 'g2a' on equation (4).

2.2 Optimised fitting formula

Up to this section, ($z \cdot E_v$) has been considered as one variable, which replaces Rea *et al.*'s CL_A. The idea is to parameterise the relation between z and E_v. The hyperbolic function of $CS(z \cdot E_v)$ compresses the small and high values of ($z \cdot E_v$), which also leads to the relatively small $RMSE$ (see Table 2).

On closer inspection, the $CS(z \cdot E_v)$ values seemed to be spreading up to $CS(z \cdot E_v) < 0.35$. Values greater than 0.35 are mathematically compressed by the hyperbolic function in equation (2), which saturates at $CS = 0.70$. To utilise these facts, E_v needs to be '*compressed*' non-linearly. Thus, an additional fitting parameter c is included in equation (2), resulting into the new fit formula for $CS(z, E_v)$ in equation (4) with two independent variables z and E_v

$$CS(z, E_v) = 0.7 - \frac{0.7}{1 + a \cdot \left(z \cdot E_v^c\right)^b} \quad (4)$$

For the following curve fitting based on equation (4), the groups are categorised into

The optimised fitting parameters a, b, c and performance measures for 'g1a' and 'g2a' are shown for the comparison in Table 2. Visually, the relationships between CS_{2018} and $CS(z, E_v)$ for both groups are shown in Figure 5. It can be seen that the accuracy of the prediction described by the parameters $\Delta CS_{|fit-pb|}$ and $|Res|_{max}$ has improved clearly for the case of group 'g1a' and for the case of group 'g2a' these changes are negligible.

This leads to the proposed model function $CS(z, E_v)$ in equation (5), after balancing prediction accuracy and formula complexity. The use of 'g2a' for the model function was omitted, since the prediction accuracy difference between 'g2a' and 'g2' is negligible

$$CS(z, E_v) = \begin{cases} 0.7 - \frac{0.7}{1 + 0.016781 \cdot \left(z \cdot E_v^{0.509265}\right)^{2.268904}}, & z > 0.195 \\ 0.7 - \frac{0.7}{1 + 0.011376 \cdot \left(z \cdot E_v\right)^{1.109998}}, & z \leq 0.195 \end{cases} \quad (5)$$

g1a: $(z > 0.195) \triangleq (SV > 0)$, data quantity: 3097

g2a: $(z \leq 0.195) \triangleq (SV \leq 0)$, data quantity: 2641

The proposed function $CS(z, E_v)$ has an inaccuracy of $\Delta CS_{|fit-pb|} = 0.036$ for (g1a: $z > 0.195$) and $\Delta CS_{|fit-pb|} = 0.033$ for (g2: $z \leq 0.195$) with prediction bounds confidence intervals of 99%.
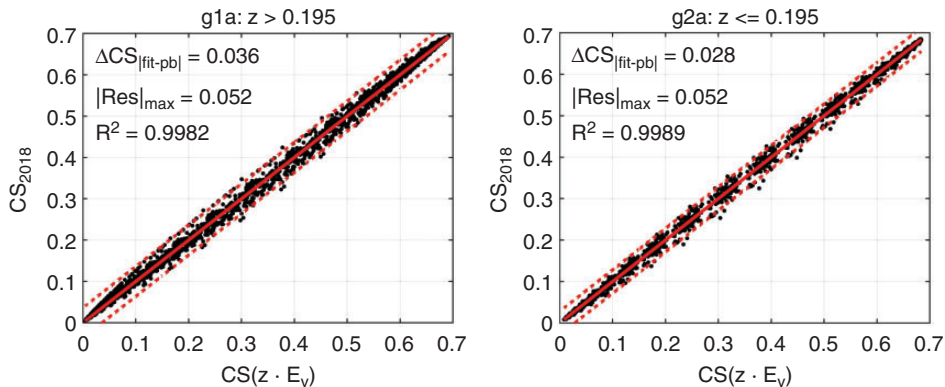

Figure 5 CS_{2018} – CS(z,Ev) plots for group 'g1a' and group 'g2a' based on equation (4)

3. Internal validation

In the last section, we have used regression analysis to create and optimise the model function $CS(z, E_v)$. In this section, an internal validation is performed to check the prediction goodness of $CS(z, E_v)$. We have chosen the method of repeated split data (RSD) described by Giancristofaro and Salmaso.[23] They reviewed diverse techniques of regression model validation and described the methodology of RSD. We adapted the method and used other performance measures to validate the proposed model:

1) *Data-splitting*: Available original data are randomly split into fitting and validation data in the ratio 3/1 ($n_{g1,fit}/n_{g1,val} = 2323/764$, $n_{g2,fit}/n_{g2,val} = 1981/660$).
2) *Model-fitting*: Fitting data are used to determine parameters after equation (2).
3) *Computation of performance measure*: The fitted model is compared with the validation data, leading to the performance measures: fitting parameters, goodness-of-fit parameters and effect size d_{Cohen}. d_{Cohen} is calculated by mean, standard deviation and sample size of fitting and validation data.[24]

4) *Iterations*: The above procedure is repeated 100 times.
5) *Interpretation of the results:* Anderson–Darling normality tests of fitting and goodness-of-fit parameter distribution. One-sample t-test comparing means of fitting and goodness-of-fit parameters with the model parameters from Table 3. Interpreting effect size distribution between fitting and validation data.

The results of RSD are shown in Table 3. The performance measures, except effect size, are tested for normality. After applying the Anderson–Darling test, all the tested performance measures follow a normal distribution ($\alpha = 0.01$, $p > 0.01$), which is a precondition for the one-sample t-test. The t-test shows that a, b, c, R^2, $_{adj}R^2$, $RMSE$ distributions have a mean equal to the corresponding values from the proposed model ($\alpha = 0.01$, $p > 0.01$, see Table 3: g1a model and g2 model). SSE is very sensitive on the sample size count by definition. Since the sample size count between the general model and iterative model is different, it is expected that the mean of SSE distribution is different to SSE of the proposed model.

Table 3 Performance measures (PM) results of RSD with 100 iterations

Parameter	g1a: z > 0.195	g1a model	g2: z ≤ 0.195	g2 model
a	0.016751 ± 0.000279	0.016781*	0.011379 ± 0.000056	0.011376*
b	2.267799 ± 0.012418	2.268904*	1.099933 ± 0.001102	1.099980*
c	0.509566 ± 0.002752	0.509265*	–	–
SSE	0.266856 ± 0.006887	0.356801**	0.228194 ± 0.006106	0.304258**
R^2	0.998247 ± 0.000052	0.998241*	0.998184 ± 0.000052	0.998183*
$_{adj}R^2$	0.998245 ± 0.000052	0.998240*	0.998183 ± 0.000052	0.998183*
$RMSE$	0.010724 ± 0.000139	0.010739*	0.010737 ± 0.000143	0.010737*
SSE_{val}	0.090206 ± 0.010788	–	0.076187 ± 0.006098	–
$RMSE_{val}$	0.006926 ± 0.000413	–	0.010735 ± 0.000433	–
$|d_{Cohen}|$	0.040 ± 0.027	–	0.033 ± 0.029	–
$max(|d_{Cohen}|)$	0.127	–	0.126	–

Note: Fitting parameters, goodness-of-fit parameters fitting and validation data (index: $_{val}$) and effect size with correspondent mean ± standard deviation are illustrated. One-sample t-test of the g1a vs. g1a model and g2 vs. g2 model with $\alpha = 0.01$ (*$p > 0.01$, **$p < 0.01$). $|d_{Cohen}|$ describes the effect between fitting and validation data distribution.

Now the effect sizes are taken into account. Under Sawilosky's and Cohen's rule of thumb, an effect $d < 0.2$ is considered very small.[24,25] A very small effect implies that testing and validation data are following the same distribution. A statistical power analysis has been performed to check what effect size can be detected with the given significance level $\alpha = 0.01$, statistical power $(1 - \beta) = 0.99$ and the sample size ratio $n_{\text{g1a,fit}}/n_{\text{g1a,val}} = 2323/764$, $n_{\text{g2,fit}}/n_{\text{g2,val}} = 1981/660$; hence, for g1a: $d_{\text{Cohen,g1a}} > 0.203562$ and g2: $d_{\text{Cohen,g2}} > 0.220461$ can be detected. In our case, the mean and standard deviation of $|d_{\text{Cohen,g1a}}|$ and $|d_{\text{Cohen,g2}}|$ are smaller than 0.2, indicating that there is a very small difference between the testing and validation groups in all 100 iteration steps. Even the maximum value of $|d_{\text{Cohen,g1a}}| = 0.125$ and $|d_{\text{Cohen,g2}}| = 0.126$ refers to a very small effect, validating the model in all 100 iterations.

In conclusion, all 100 fitting models are validated and since the means of the fitting parameters a, b and the goodness-of-fit parameters R^2, $_{\text{adj}}R^2$, $RMSE$ are equal to the corresponding values from the proposed model (see Table 3), the proposed model in equation (5) can be used to predict CS_{2018} values.

4. External validation

In addition, the proposed model is validated externally, using absolute spectral power distributions measured in a typical German industry hall (50.870°, 8.605°). The industrial hall used a combination of tubular fluorescent lamps, LED light sources (both with: $CCT = 4000\,\text{K}$ and $R_{\text{a}} > 80$) and natural daylight to illuminate the workplaces. During whole working time (5:30 a.m. – 2:00 p.m.), the lighting system was on and was not dimmed.

Starting from 26 March 2019 until 26 April 2019, the vertical spectral irradiance at eye level of industrial workers (height $h = 1.5\,\text{m}$) was recorded every 15 min with an ILT560A spectrometer (optical bandwidth: 1.5 nm, wavelength range: 380 nm – 780 nm) and a W-diffusor (input optic). Figure 6 shows four absolute spectral power distributions recorded by the spectrometer during working hours on 28 March 2019. The spectrometer position and detector direction within the industrial hall can be seen on the floor plan in Figure 7. Once in the night without daylight on the date 28 March 2019, four measurements with a reference incandescent lamp were performed. For the validation and computation of CS_{2018}, z and E_{v} only absolute spectra with $E_{\text{v}} > 1\,\text{lx}$ were used ($n = 2185$).
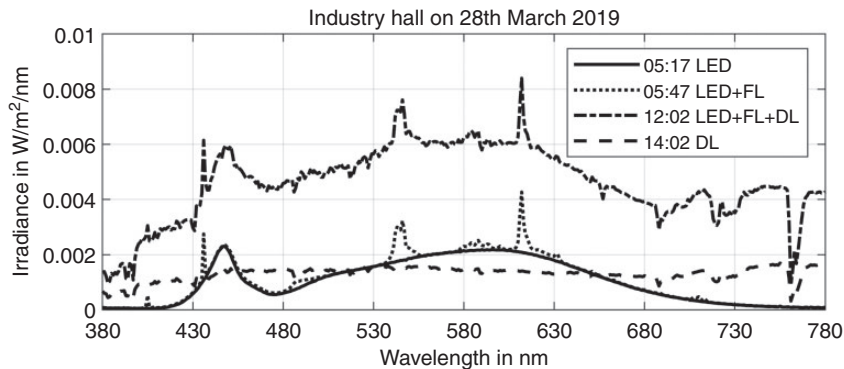
Figure 6 Four absolute spectral power distributions measured during the working times. (LED: light-emitting diode; FL: fluorescent lamp; DL: daylight)
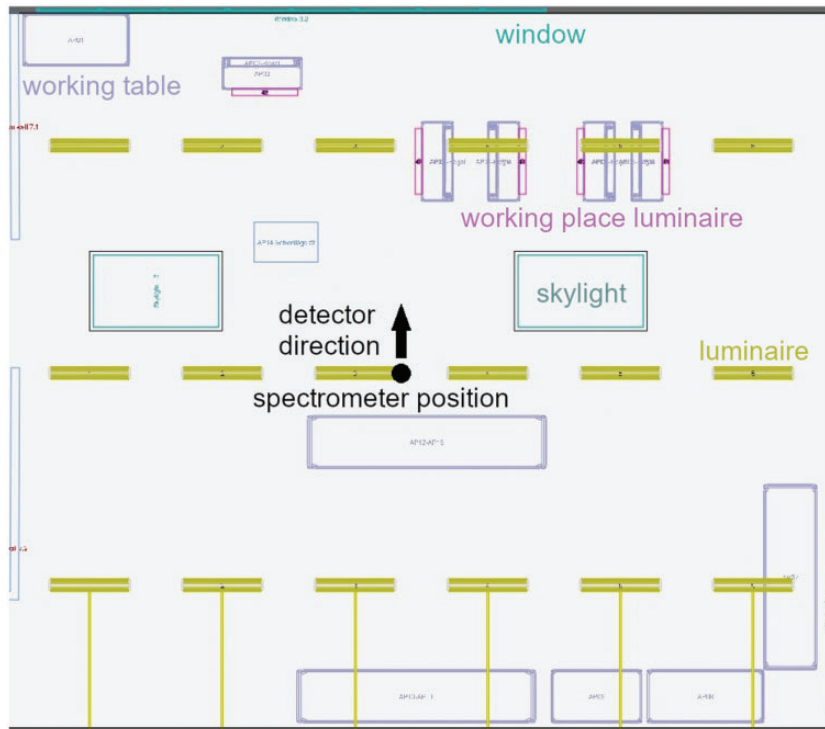
Figure 7 Floor plan of the industry hall including position of skylights, luminaires, working tables, windows and spectrometer

Comparing if-condition (0.195 – z) with if-condition SV in Figure 8 shows a valid separation of the positive and negative SV values in group g1a (n = 2181) and in group g2 (n = 4). Notably, the four measurements in group g2 were recorded with the above mentioned incandescent lamp.

Now comparing the performance measures SSE, R^2, $RMSE$ and $|Res|_{max}$ with the proposed g1a and g2 models from Table 2, shows that the model function $CS(z, E_v)$ only makes a slight error by estimating the CS_{2018}, see $RMSE$ and $|Res|_{max}$ in Table 4.

5. Discussion

In the last sections, Rea and Figueiro's model of CS from 2018 has been analysed and a

model function $CS(z, E_v)$ has been created to compute the quantity CS_{2018} based on the chromaticity coordinate z (CIE, observation angle 2°) and illuminance (E_v). Then, Rea's if-condition (SV) was applied by finding a corresponding if-condition dependent on z to improve the prediction accuracy of $CS(z, E_v)$. The proposed model function in Equation (5) was validated internally with the evaluation of the distribution of effect size d_{Cohen}, fitting and goodness-of-fit parameters. Additionally, the external validation of $CS(z, E_v)$ using measured absolute spectra was performed in a typical German industrial hall.

However, there are also some limitations in the proposed model. Since this model was created with white light spectra only, it should not be used on monochromatic light sources. As already mentioned, the database for the

Table 4 Goodness-of-fit statistics between CS_{2018} and $CS(z, E_v)$ from the external validation (g1a: $z > 0.195$, g2: $z \leq 0.195$) and proposed models (g1a model, g2 model)

Parameter	g1a: $z > 0.195$	g1a model	g2: $z \leq 0.195$	g2 model
SSE	0.573673	0.356801	0.003835	0.304258
R^2	0.998742	0.998241	0.999503	0.998183
RMSE	0.016218	0.010739	0.028211	0.010737
$|Res|_{max}$	0.026	0.052	0.030	0.058
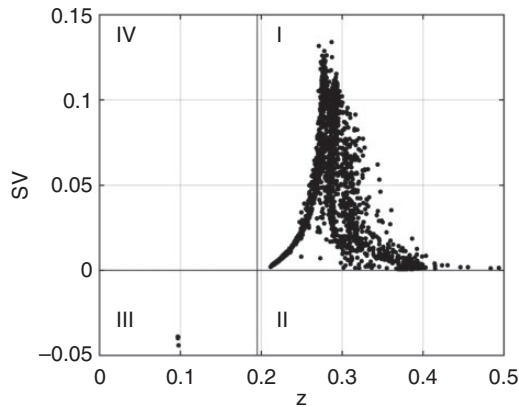
Figure 8 Relationship between z and SV with 2185 absolute spectra measured in the field. The borderline at $z = 0.195$ is separating positive and negative SV values

fitting in this work is mainly represented by LED light sources, so the validity for other light source types may be limited.

In summary, the proposed model function $CS(z, E_v)$ can predict Rea's quantity CS_{2018} with acceptable errors for white light sources ($|Res|_{max} < 0.058$). This model should only be applied with white light sources and in the illuminance range 10 lx–10,000 lx. Nonetheless, the $CS(z, E_v)$ model is an alternative for lighting practitioners and researchers to evaluate circadian-effective light on humans, when only a colorimeter is available and when it is not possible to invest in a suitable spectrometer. Since $CS(z, E_v)$ is calculated with a relatively simple formula, using only chromaticity coordinate z and illuminance E_v, cost-effective colour sensors could also be used to measure and determine the value CS_{2018}. In order to extend and verify

the potential of the proposed model for limited functional devices such as low-cost colour sensors or chromatic measurement devices, many measurements, experiments and validations need to be undertaken.

Declaration of conflicting interests

The authors declared no potential conflicts of interest with respect to the research, authorship, and/or publication of this article.

ORCID iDs

W Truong   (iD)   https://orcid.org/0000-0002-9857-4437
V Trinh (iD) https://orcid.org/0000-0002-1390-5322

References

1 Commission Internationale de l'Eclairage. CIE *015:*2018. *Colorimetry*. Vienna: CIE, 2018.

2 Commission Internationale de l'Eclairage. CIE S 026/E:2018. *CIE System for Metrology of Optical Radiation for ipRGC-lnfluenced Responses to Light*. Vienna: CIE, 2018.

3 Deutsches Institut fur Normung. DIN SPEC 5031-100. *Strahlungsphysik im optischen Bereich und Lichttechnik – Teil 100: Über das Auge vermittelte, melanopische Wirkung des Lichts auf den Menschen*. Berlin: DIN, 2015.

4 Deutsches Institut fur Normung. DIN SPEC 67600. *Biologisch wirksame Beleuchtung - Planungsempfehlungen*. Berlin: DIN, 2013.

5 Lucas RJ, Peirson SN, Berson DM, Brown TM, Cooper HM, Czeisler CA, Figueiro MG, Gamlin PD, Lockley SW, O'Hagan JB, Price LL, Provencio I, Skene DJ, Brainard GC. Measuring and using light in the melanopsin age. *Trends in Neuroscience* 2014; 37: 1–9.

6 Rea MS, Figueiro MG, Bullough JD, Bierman A. A model of phototransduction by the human circadian system. *Brain Research Reviews* 2005; 50: 213–228.

7 Rea MS, Figueiro MG, Bierman A, Bullough JD. Circadian light. *Journal of Circadian Rhythms* 2010; 8: 2.

8 Rea MS, Figueiro MG, Bierman A, Hamner R. Modelling the spectral sensitivity of the human circadian system. *Lighting Research and Technology* 2012; 44: 386–396.

9 Rea MS, Figueiro MG. Light as a circadian stimulus for architectural lighting. *Lighting Research and Technology* 2018; 50: 497–510.

10 Fotios SA, Levermore GJ. Chromatic effect on apparent brightness in interior spaces II: SWS lumens model. *Lighting Research and Technology* 1998; 30: 103–106.

11 Rea MS, Mou X, Bullough JD. Scene brightness of illuminated interiors. *Lighting Research and Technology* 2016; 48: 823–831.

12 Khanh TQ, Bodrogi P, Guo X, Phan QA. Towards a user preference model for interior lighting. Part 2: experimental results and modelling. *Lighting Research and Technology* 2019; 51: 1030–1043.

13 Khanh TQ, Bodrogi P, Guo X, Phan QA. Towards a user preference model for interior lighting Part 1: Concept of the user preference model and experimental method. *Lighting Research and Technology* 2019; 51: 1014–1029.

14 Figueiro MG, Kalsher M, Steverson BC, Heerwagen J, Kampschroer K, Rea MS. Circadian-effective light and its impact on alertness in office workers. *Lighting Research and Technology* 2019; 51: 171–183.

15 Figueiro MG, Plitnick BA, Lok A, Jones GE, Higgins P, Hornick TR, Rea MS. Tailored lighting intervention improves measures of sleep, depression, and agitation in persons with Alzheimer's disease and related dementia living in long-term care facilities. *Clinical Interventions in Aging* 2014; 9: 1527–1537.

16 Figueiro MG, Rea MS. Office lighting and personal light exposures in two seasons: impact on sleep and mood. *Lighting Research and Technology* 2016; 48: 352–364.

17 Figueiro MG, Steverson B, Heerwagen J, Kampschroer K, Hunter CM, Gonzales K, Plitnick B, Rea MS. The impact of daytime light exposures on sleep and mood in office workers. *Sleep Health* 2017; 3: 204–215.

18 Moore RY. Suprachiasmatic nucleus in sleep-wake regulation. *Sleep Medicine* 2007; 8 Suppl 3: 27–33.

19 Kantermann T, Juda M, Merrow M, Roenneberg T. The human circadian clock's seasonal adjustment is disrupted by daylight saving time. *Current Biology* 2007; 17: 1996–2000.

20 Roenneberg T, Daan S, Merrow M. The art of entrainment. *Journal of Biological Rhythms* 2003; 18: 183–194.

21 Rüger M, St Hilaire MA, Brainard GC, Khalsa SB, Kronauer RE, Czeisler CA, Lockley SW. Human phase response curve to a single 6.5 h pulse of short-wavelength light. *Journal of Physiology* 2013; 591: 353–363.

22 Khalsa SBS, Jewett ME, Cajochen C, Czeisler CA. A phase response curve to single bright light pulses in human subjects. *Journal of Physiology* 2003; 549: 945–952.

23 Giancristofaro RA, Salmaso L. Model performance analysis and model validation in logistic regression. *Statistica* 2003; 63: 375–396.

24 Cohen J. *Statistical Power Analysis for the Behavioral Sciences*. 2nd ed, Hillsdale, NJ: Erlbaum, 1988.

25 Sawilowsky SS. New effect size rules of thumb. *Journal of Modern Applied Statistical Methods* 2009; 8: 597–599.